High-Power Terahertz Waves from $Bi_2Sr_2CaCu_2O_{8+d}$ Mesas

F. Turkoglu[1], H. Koseoglu[1], Y. Demirhan[1], L. Ozyuzer[1], S. Preu[2], S. Malzer[2], Y. Simsek[3], P. Müller[3], T. Yamamoto[4] and K. Kadowaki[4]

[1]Department of Physics, Izmir Institute of Technology, 35430 Urla Izmir, Turkey,
[2]Chair of Applied Physics, University of Erlangen-Nurnberg, Erlangen, Germany
[3]Physical Institute III, University of Erlangen-Nurnberg, Erlangen, Germany
[4]Institute of Materials Science, University of Tsukuba, Tsukuba, Japan

E-mail: ozyuzer@iyte.edu.tr

Keywords: Intrinsic Josephson Junctions, Terahertz radiation, $Bi_2Sr_2CaCu_2O_{8+\delta}$ (Bi2212) single crystal

We fabricated rectangular mesa structures of superconducting $Bi_2Sr_2CaCu_2O_{8+\delta}$ (Bi2212) using e-beam lithography and Ar ion beam etching techniques for terahertz (THz) emission. C-axis resistance versus temperature (R-T), current-voltage (I-V) characteristics and bolometric THz power measurements were performed to characterize Bi2212 mesas. The emission frequency of mesas was determined using a simple Michelson interferometer set up which also demonstrates polarized emission. Interference patterns of THz radiation from Bi2212 mesas were detected by various detectors such as a liquid Helium cooled silicon composite bolometer, a Golay cell and a pyroelectric detector. An emitted power as high as 0.06 mW was detected from Bi2212 mesas. This is the first time, most of the pumped power was extracted as THz emission from a Bi2212 mesa. The radiation was at 0.54 THz determined using the Michelson interferometric setup.

Corresponding Author: Lutfi Ozyuzer

E-mail: ozyuzer@iyte.edu.tr
Address: Dept. of Physics,
Izmir Institute of Technology
Gulbahce Campus, Urla
35430 Izmir, Turkey

Phone: +90 232 750 7705
Fax : +90 232 750 7707

Although electromagnetic waves in the terahertz frequency region (0.1 to 10 THz) host potential applications including sensing, imaging and spectroscopy, these applications are presently limited by the lack of powerful, continuous wave, and compact solid-state sources [1,2]. The Josephson effect, occurring between two superconductors separated by a thin insulating layer, provides a unique and simple principle to generate electromagnetic radiation in the terahertz frequency range. When a dc voltage is applied across the junction, an ac-current oscillates at the Josephson frequency $f_{Jos}= V/\Phi_0$, where V is the voltage across the junction and Φ_o is flux quantum. For instance, 1 mV corresponds to an emission frequency of 0.483 THz. Therefore, Josephson junctions are potential sources of high-frequency electromagnetic radiation. Unfortunately, the operation frequency of the Josephson oscillator fabricated out of conventional superconductors is limited by the small superconducting energy gap [3]. Furthermore, the typical observed emission power is in the range of picowatts for a single junction. The emitted power can be enhanced using a large mutually coherent array of Josephson junctions made of conventional superconductors with various synchronization methods; however, variations of junction parameters may cause desynchronization and significant drop in emission power [4].

Stacks of intrinsic Josephson junctions (IJJ) in layered high temperature superconductors, such as $Bi_2Sr_2CaCu_2O_{8+\delta}$ (Bi2212), offer the most promising alternative for terahertz oscillators. Since the junctions are homogeneous on the atomic scale along the c-axis of Bi2212 single crystals, a very high density of IJJs (one junction per 1.5 nm) makes the super-radiation possible with many junctions. Moreover, a large superconducting gap of 40 meV [5] allows for high Josephson frequencies up to 15 THz. However, the major issue to synchronize oscillations in all junctions also remains for Bi2212 system. To excite coherent electromagnetic radiation from intrinsic Josephson junctions, many approaches have been considered, among them the method of using moving Josephson vortices oscillating charge was investigated most intensively [6]. Nevertheless, high-frequency emission was observed up to 0.5 THz from Bi2212 with a weak power due to unsynchronized Josephson oscillations [7].

Recently, we observed continuous, coherent and monochromatic electromagnetic terahertz radiation emitted along the walls of rectangular mesa-shaped samples of the high temperature superconductor Bi2212. The mesa acts as electromagnetic cavity, synchronizing almost all of the IJJ [8]. We observed that the fundamental frequencies of the emission were as high as 0.85 THz for a mesa width of 40 μm providing an emitted power of up to 0.5 μW. More recently, emitted powers of 5 μW and frequencies at the higher harmonics up to 2.5 THz have been obtained [9]. The thermal management of the large mesas on Bi2212 crystals has been investigated by Kurter et al. [10]. Furthermore, they showed that the backbending in the I-V curve results from the particular temperature dependence of quasiparticle resistances for Bi2212

rather than a significant suppression of the energy gap. Angular dependence of the emission power has also been studied [11]. Wang et al. imaged electric field distributions in the junction stack of Bi2212 by low temperature scanning laser microscopy and observed standing electromagnetic waves (cavity resonances)[12]. They found that standing waves of the electric field are created through interactions with a hot spot and this effect may have an active role in generating synchronized radiation from intrinsic Josephson junction stacks. In ref. [13] we discussed the dependence of the characteristics of the mesa structures on the oxygen doping level of the Bi2212 crystals and reported that the THz emitting mesas are below a certain underdoped level, which has relatively small critical current in contrast to optimally doped and overdoped Bi2212. Minami, et al. reported the radiation characteristics of terahertz radiation emitted from rectangular mesa structures of Bi2212 and they concluded that these devices exhibit enough frequency purity, intensity, and controllability suitable for device applications [14]. By improving the sample fabrication technique, Yamaki et al. estimated total emission power of Bi2212 mesa structures about 30 μW [15].

Many theoretical models have been proposed to explain the nature of the mechanism of THz emission from Bi2212 mesas. Koshelev and Bulaevskii proposed that modulations of the Josephson critical current along the width of mesa is responsible for the cavity resonance [16]. A new dynamic state caused by the nonlinear property of IJJ has been discovered in which the phase kinks enable cavity resonance modes of the Josephson plasma [17,18]. Tachiki et al. suggest that the energy of the nonradiative component of the magnetic field allows determining the orientation of the cavity resonance mode [19]. However, there is no consensus about the precise nature of the synchronization mechanism.

In this study, single crystals of Bi2212 grown by traveling solvent floating zone technique (TSFZ) method were used. The as grown crystals were cut in small pieces and annealed in partial O_2 pressure with slow and long processes for two days to obtain homogenous underdoped Bi2212 single crystals. After annealing, a piece of a small single crystal was glued on a sapphire substrate with silver epoxy. The crystals were cleaved using a scotch tape and then a 100 nm gold film was evaporated onto the crystal. A mesa patterning process followed, allowing to apply a voltage and measure the current–voltage (I-V) characteristics along the c-axes of the Bi2212. Rectangular mesa structures (55 x 300 μm^2) with a height of 1250 nm were fabricated on Bi2212 single crystals using e-beam lithography and Ar ion beam etching techniques. After the mesa fabrication, a CaF_2 layer was evaporated through a shadow mask onto the top part of the crystal, including a small section of the mesa for the electrical isolation purpose, in order to establish electrical contact to the gold layer on top of the mesa,. Lift off technique was used for fabrication of gold stripes by e-beam lithography onto the mesa and the CaF_2. Finally, a gold wire was attached to the gold strip over the CaF_2 and two pads with silver epoxy for the electrical contacts of the mesa and two pads.

In order to characterize the Bi2212 mesas, c-axis resistance versus temperature (R-T) and I-V behavior were measured in a He flow cryostat. During I-V characterization, the emission characteristics of the mesas below T_c were also measured with a bolometer, Golay cell or a pyroelectric detector. A Michelson interferometer set up as shown in Fig. 1 was used to determine the emission frequency. First, a complete I-V curve is measured with one blocked mirror of Michelson interferometer. The optimum emission voltage is obtained from these data. Then, the mesa is biased at this voltage and interferometric data were taken.

Figure 2(a) shows the I−V curve of one of the representative THz emitting mesas with 55x300 μm^2 at T=35 K. The trace was taken by both a back and forward scan. A large contact resistance between gold and Bi2212 is determined from the I-V curve. The data also shows that the Josephson current density is 103 A/cm^2 which is in the underdoped region of Bi2212 phase diagram and comparable to other THz emitting mesas [13]. Figure 2(b), shows the detected THz radiation signals from a Si composite bolometer. The bolometer signal is increasing at back bending region of I-V curve. It indicates that local temperature of the mesa is increasing and the bolometer detects the heating of the mesa in the form of unpolarized, incoherent blackbody radiation. When all junctions are in the resistive state and the bias is decreasing slowly, polarized and synchronized emission peaks from the mesa for positive and negative bias voltages were observed in the return branches at ± 1.28 V. On the bias decreasing part of the I-V curve at low bias there are some jumps (Fig. 2(a)). They occur as some junctions switch to the zero voltage state and they are referred to as re-trapping. When we look at the emission region (arrows in Fig. 2(a)), we see a bump in the return branch due to radiation (inset of Fig. 2(a)). That is, emission persists over an extended voltage range around the resonance condition. This property is a consequence of the slightly inclined side walls of the mesa resonator and allows for the design of THz sources with voltage-tunable emission frequencies [20]. As it can be seen from the close-up of the return branch, no re-trapping events were observed in the emission region, indicating that all junctions are tightly locked to the resistive state. The absence of a jump in the I-V curve allows us to establish a baseline of the current and to determine the excess current that supplies the energy for the excitation of the cavity resonance. These data suggest that about 126 μW are pumped into the in-phase resonance.

The frequency of the emission was determined by a simple interferometer set up as shown in Fig. 1 implementing various detectors (bolometer, Golay cell and pyroelectric detector). The setup splits a single wave emitted from the long edge of mesa so that one wave strikes a fixed mirror and the other a movable mirror. When the reflected beams are brought together, they form an interference pattern proving the coherence. The interference patterns were detected outside of the cryostat after traveling a long way through ambient air with high losses.

Figure 3 shows signals detected by the detectors in the interferometer setup. It can be clearly seen that signals detected by Si composite bolometer has lower noise due to its higher sensitivity. Our bolometer has 10^{-13} W/Hz^{½} NEP value but has to work under liquid-helium-temperature. The cryogenic environment is not necessary for the Golay cell and the pyroelectric detector, but, their sensitivities are much lower than Si composite bolometer. The NEP values are in the range of 1 nW/Hz^{½} for Golay cell and 60 nW/Hz^{½} for pyroelectric detector; therefore, more noisy signals were observed from pyroelectric detector. However, radiation could even be detected with the pyroelectric detector is the proof of intense radiation.

The emission frequency was calculated by fast Fourier transform (FFT) of interference data given in Fig. 3 using Labview program. Figure 4 shows the Fourier transform of the data, providing the frequency spectrum of the emission. The peak in this figure indicates that the emission frequency is 0.54 THz for all three different detector setups. The noise in interferometer patterns of pyroelectric detector also shows noise in FFT spectrum. If we subtract the contact resistance from I-V curve, the voltage of the bump decreases to 955 mV. According to the Josephson voltage-frequency relation, emission frequency is 0.54 THz which occurs at 955 mV for 833 junctions. This is consistent with interferometer result, so it satisfies Josephson voltage-frequency relation.

In order to estimate emission power, firstly we calculated the signal to noise ratios from Fig. 4 and then we determined the irradiance incident on the detectors using,

$$H = \frac{NEP}{A}\left(\frac{V_s}{V_n}\right)(\Delta f)^{1/2} \qquad (1)$$

where H is the irradiance incident on the detector of area A, V_n is the root mean square noise voltage within the measurement bandwidth Δf, and V_s is the root mean square signal voltage [21]. We get nearly 270 nW emission power for Golay cell an pyroelectric detector for 1 Hz band width. This leads to a value of 60 µW total power when we take into account the geometrical configurations of the mesa and equipments. Since the pumped power is 126 µW, 47.6 % of the total dc power is dissipated in the mesa. To the knowledge of the authors, this is the first time, that most of the pumped power is extracted as THz emission. The emitted power could be further improved by improving experimental techniques such as increasing annealing time to obtain more homogenous doping of underdoped Bi2212 single crystals. We note that the emitted power might still be underestimated since the frequency of 0.54 THz is very close to a water vapor absorption line and the setup was in ambient air.

THz detection from rectangular Bi2212 mesa structures nowadays is mostly accomplished with bolometers. In this paper, we showed that synchronously emitting Josephson

junctions from Bi2212 provide sufficient power to use room temperature THz detectors, such as Golay cells and pyroelectric detectors due to the high emitted power. We calculate that most of the pumped power is extracted as THz emission. In contrast to previous studies, the emission frequency was determined using interferometer set up instead of FTIR. The interference patterns were detected after traveling a long way through ambient air. The emission frequency calculated by a Fourier transformation of the interference data is consistent with Josephson frequency-voltage relation. These THz emitting mesas can easily be used for practical applications as sub-THz sources without the need for high magnetic fields as in case of moving vortices or sub-THz operation of quantum cascade lasers (QCL) [2].

This research is supported in part by the TUBITAK (Scientific and Technical Council of Turkey) project number 110T248. L. Ozyuzer acknowledges support from the Alexander von Humboldt foundation.

[1] M. Tonouchi, Nature Photonics **1**, 97 (2007).

[2] S. Preu, G. H. Döhler, S. Malzer, L.J. Wang and A.C. Gossard, J. Appl. Phys. **109**, 061301 (2011).

[3] D. N. Langenberg, D. J. Scalapino, B. N. Taylor and R. E. Eck, Phys. Rev. Lett. **15**, 294 (1965).

[4] P. Barbara, A. B. Cawthorne, S. V. Shitov and C. J. Lobb, Phys. Rev. Lett. **82**, 1963 (1999).

[5] L. Ozyuzer, J. F. Zasadzinski , N. Miyakawa, Int. J. Mod. Phys. B **13**, 3721 (1999)

[6] M. H. Bae, H. J. Lee and J. H. Choi, Phys. Rev. Lett. **98**, 027002 (2007).

[7] I. E. Batov, X. Y. Jin, S. V. Shitov, Y. Koval, P. Müller and A. V. Ustinov, Appl. Phys. Lett. **88**, 262504 (2006).

[8] L. Ozyuzer, A. E. Koshelev, C. Kurter, N. Gopalsami, Q. Li, M. Tachiki, K. Kadowaki, T. Yamamoto, H. Minami, H. Yamaguchi, T. Tachiki, K. E. Gray, W. K. Kwok and U. Welp, Science **318**, 1291 (2007).

[9] K. Kadowaki, H. Yamaguchi, K. Kawamata, T. Yamamoto, H. Minami, I. Kakeya, U. Welp, L. Ozyuzer, A. E. Koshelev, C. Kurter, K. E. Gray and W. K. Kwok, Physica C **468**, 634 (2008).

[10] C. Kurter, K. E. Gray, J. F. Zasadzinski, L. Ozyuzer, A. E. Koshelev, Q. Li, T. Yamamoto, K. Kadowaki, W. K. Kwok, M. Tachiki and U. Welp, IEEE Trans. Appl. Superconductivity **19**, 428 (2009).

[11] K. Kadowaki, M. Tsujimoto, K. Yamaki, T. Yamamoto, T. Kashiwagi, H. Minami, M. Tachiki, and R. A. Klemm, J. Phys. Soc. Jpn. **79**, 023703 (2010).

[12] H. B. Wang, S. Guenon, J. Yuan, A. Iishi, S. Arisawa, T. Hatano, T. Yamashita, D. Koelle and R. Kleiner, Phys. Rev. Lett. **102**, 017006 (2009).

[13] L. Ozyuzer, Y. Simsek, H. Koseoglu, F. Turkoglu, C. Kurter, U. Welp, A. E. Koshelev, K. E. Gray, W. K. Kwok, T. Yamamoto, K. Kadowaki, Y. Koval, H. B. Wang and P. Müller, Supercond. Sci. and Technol. **22**, 114009 (2009).

[14] H. Minami, I. Kakeya, H. Yamaguchi, T. Yamamoto and K. Kadowaki, Appl. Phys. Lett. **95 (23)**, 232511 (2009).

[15] K. Yamaki, M. Tsujimoto, T. Yamamoto, A. Furukawa, T. Kashiwagi, H. Minami, and K. Kadowaki, Opt. Express **19**, 3193-3201 (2011) .

[16] A. E. Koshelev and L. N. Bulaevskii, Phys. Rev. B **77**, 014530 (2008).

[17] S. Lin, X. Hu and M. Tachiki, Phys. Rev. B **77**, 014507 (2008).

[18] S. Lin and X. Hu, Phys. Rev. Lett. **100**, 247006 (2008).

[19] M. Tachiki, S. Fukuya, and T. Koyama, Phys. Rev. Lett. **102**, 127002 (2009).

[20] K.E. Gray, L. Ozyuzer, A.E. Koshelev, C. Kurter, K. Kadowaki, T. Yamamoto, H. Minami, H. Yamaguchi, M. Tachiki, W.K. Kwok and U. Welp, IEEE Transactions on Applied Superconductivity **19**, 886 (2009).

[21] J. Ready, Module 1.6, p. 211, Fundamentals of Photonics Ed. C. Roychoudhuri, SPIE Press (Bellingham, 2011)

Figure Captions

Figure 1. Michelson interferometer setup for frequency determination of mesas.

Figure 2. (a) Current versus Voltage (I-V) curve of the mesa at 28 K. The inset shows detailed demonstration of bump at emission voltage. Note that contact resistance is subtracted from I-V curve to find exact pump energy. (b) LHe cooled Si composite Bolometer versus Voltage curve of the mesa at 35 K.

Figure 3. Interference patterns detected by bolometer, Golay cell and pyroelectric detector.

Figure 4. Fast Fourier Transforms of interference patterns given in Fig. 3.

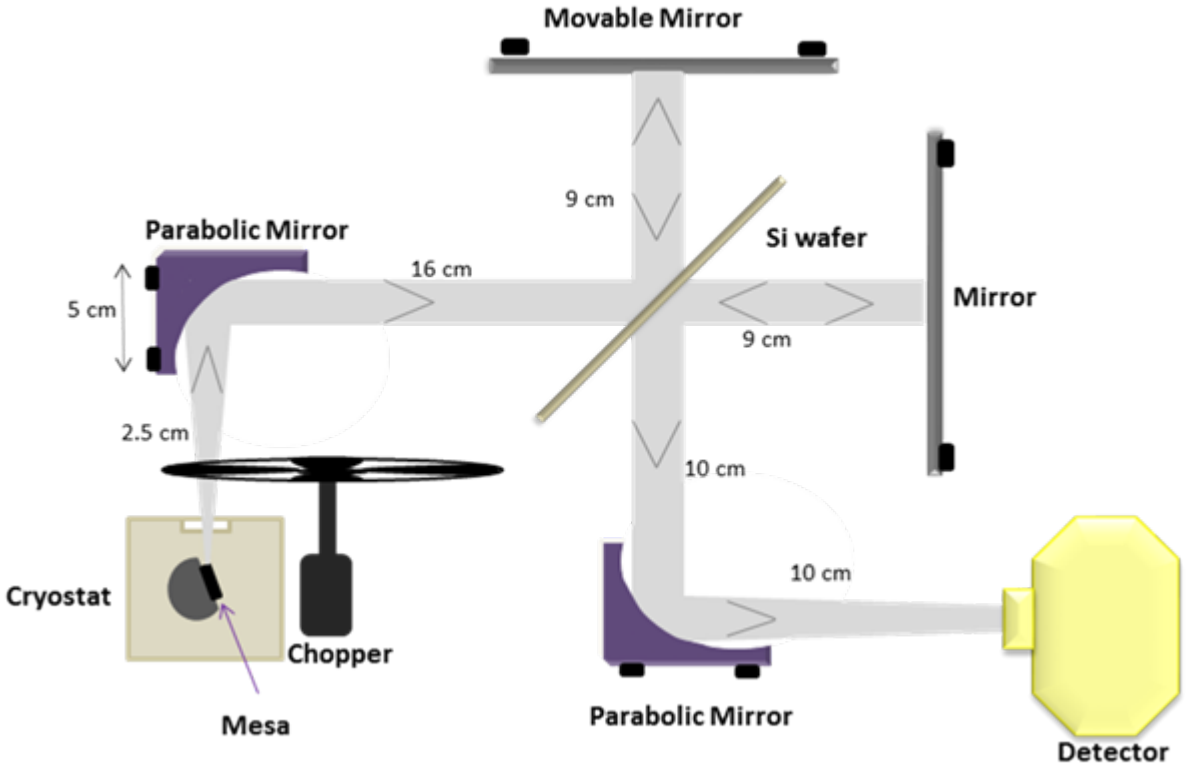

Figure 1
Ozyuzer et al.

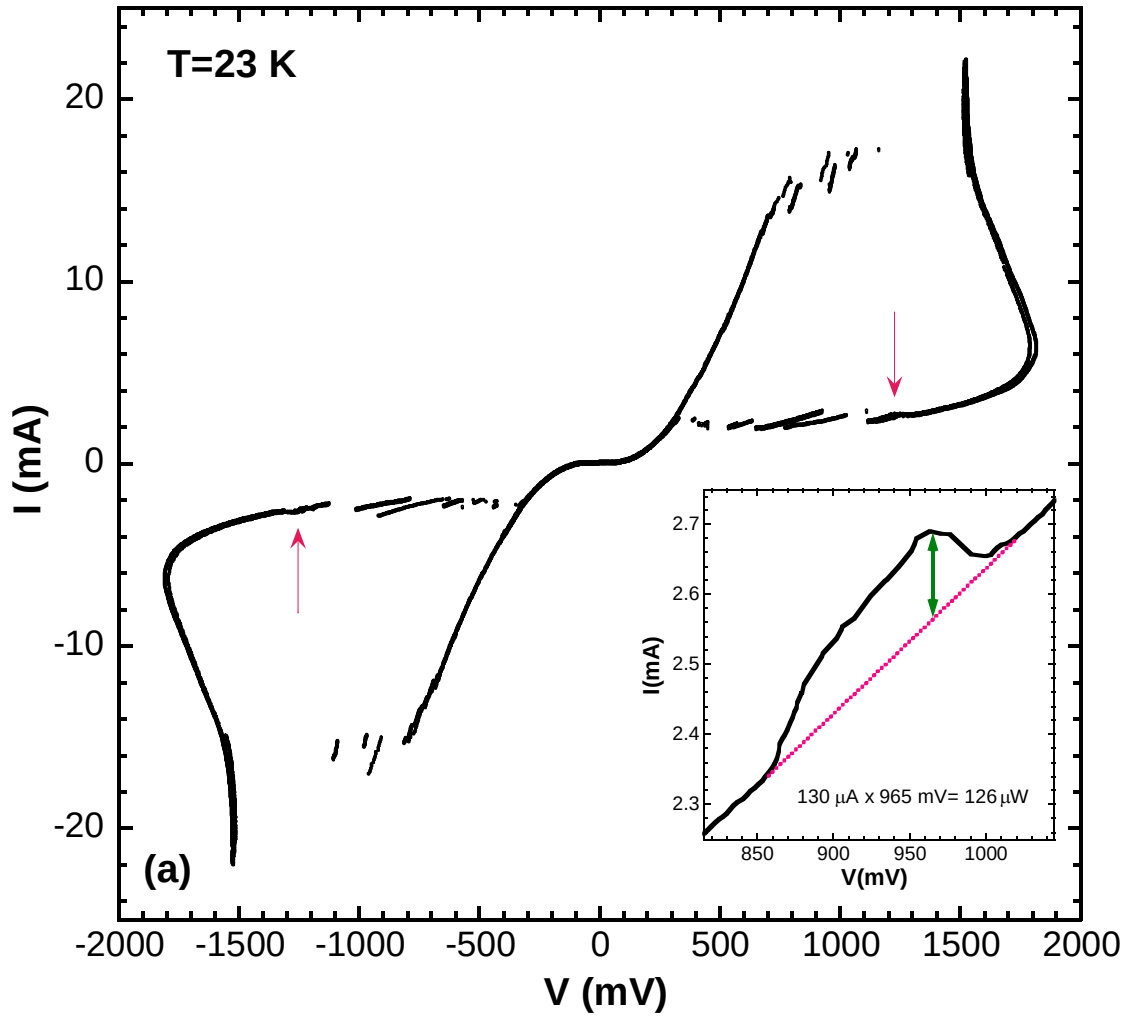

Figure 2(a)
Ozyuzer et al.

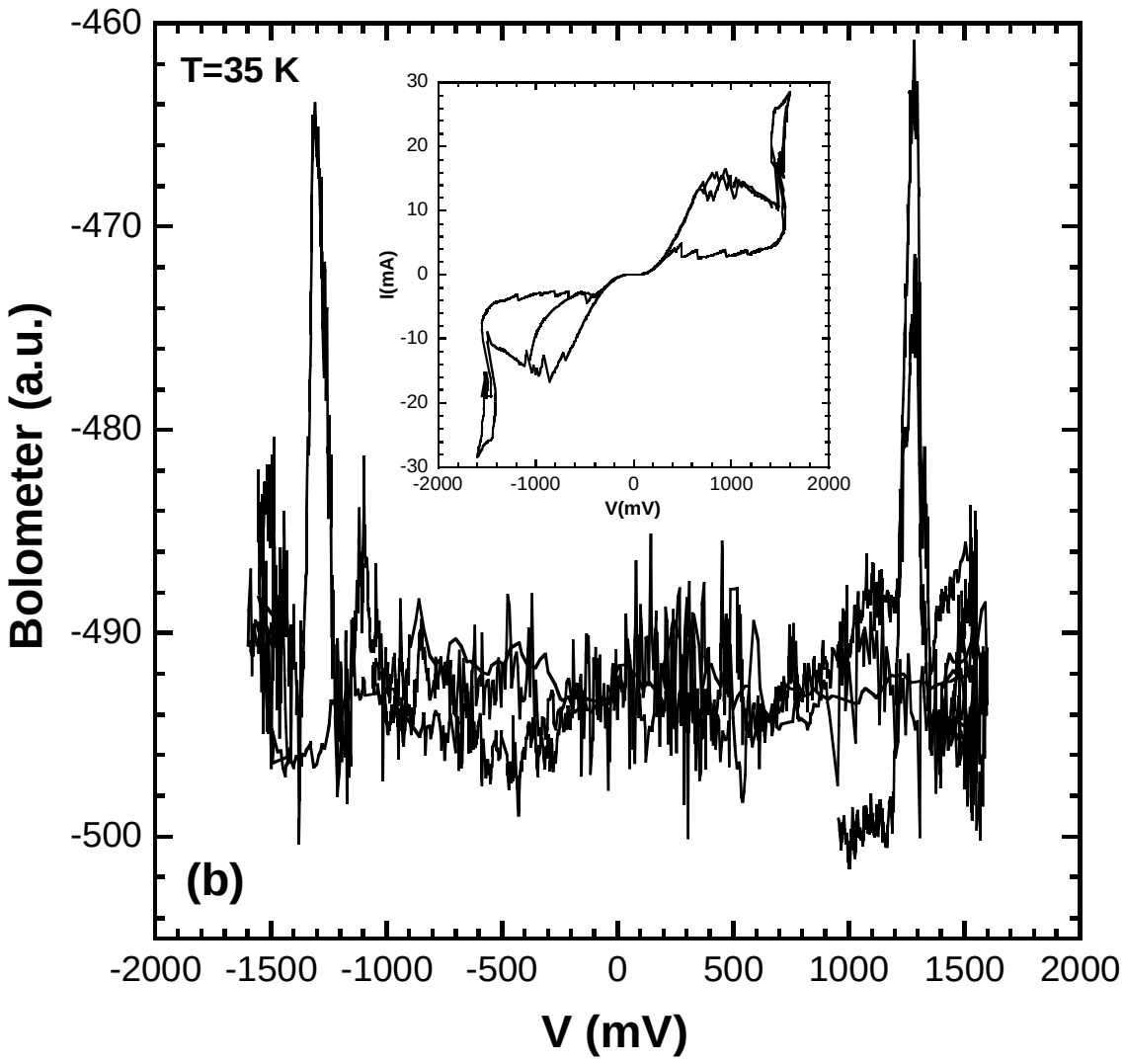

Figure 2(b)
Ozyuzer et al.

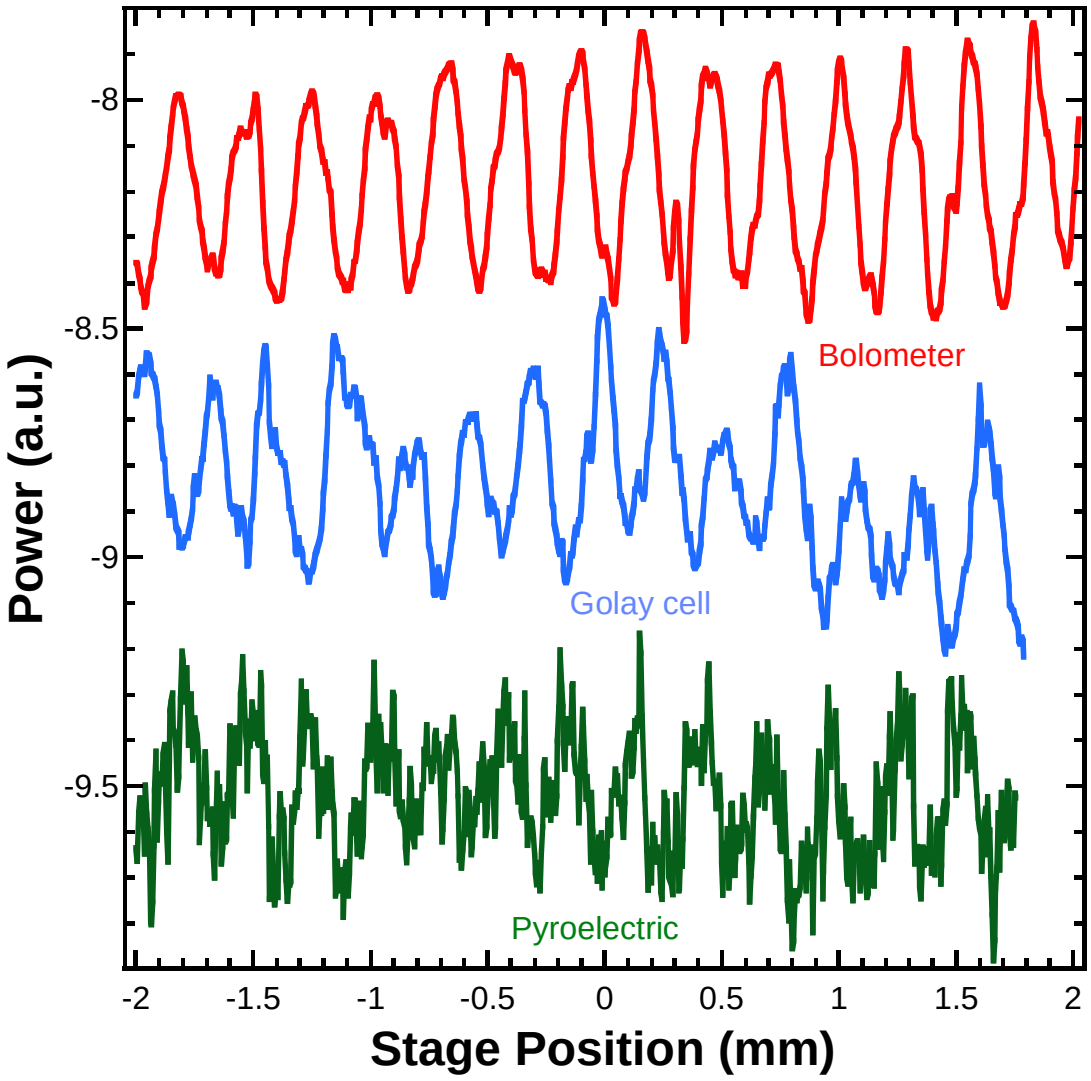

Figure 3
Ozyuzer et al.

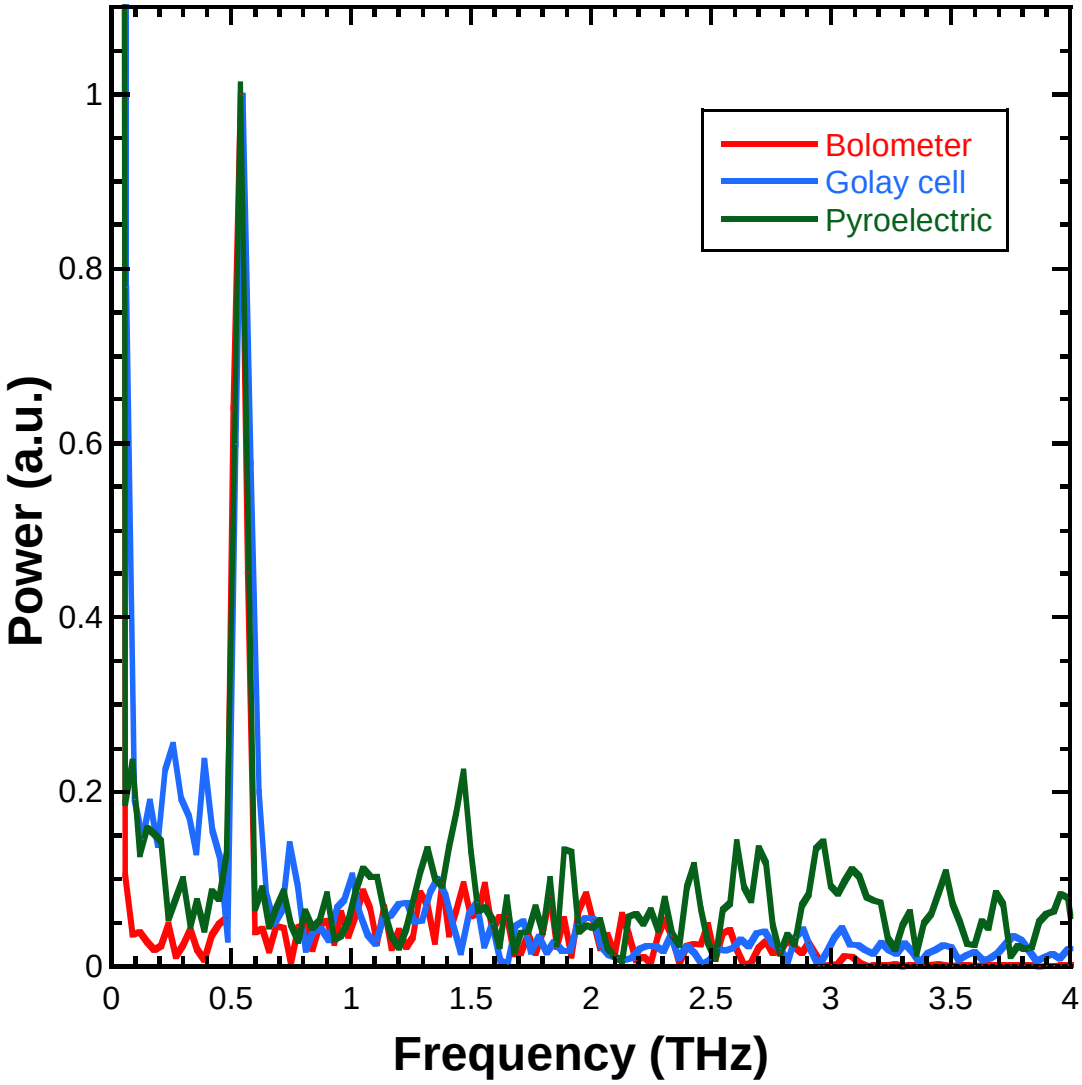

Figure 4
Ozyuzer et al.